An explicit reduced mechanism for H_2-air combustion

P. Boivin[a], C. Jiménez[a,b], A. L. Sánchez[a], F.A. Williams[c]

[a]*Dept. Ingeniería Térmica y de Fluidos, Universidad Carlos III de Madrid, Leganés 28911, Spain*
[b]*Dept. Combustibles Fósiles, Centro de Investigaciones Energéticas, Medioambientales y Tecnológicas, Madrid, Spain*
[c]*Dept. of Mechanical and Aerospace Engineering, University of California San Diego, La Jolla CA 92093-0411, USA*

Abstract

For hydrogen-oxygen-inert systems, just as for other fuel-oxidizer mixtures, systematically reduced chemistry has in the past been developed separately for premixed and diffusion flames and for autoignition. In computational work that addresses turbulent combustion or the transition from deflagration to detonation, however, autoignition and flames both may occur, and reduced chemistry may be required because of computer limitations. To fill that need, systematically reduced chemistry is presented here that encompasses autoignition and flames. The description involves three global steps among five reacting species, H_2 , O_2 , H_2O, H and HO_2, being based on approximations to chemical-kinetic steady states for O, OH and H_2O_2. These steady states apply well under all conditions except during autoignition in lean and stoichiometric mixtures, where they underpredict induction times substantially. To remedy this deficiency, which occurs only when HO_2 is not in steady state, an autoignition analysis is employed to derive a correction factor that reduces the value of the specific reaction-rate constant for the branching step $H+O_2 \rightarrow OH+O$, used in the three-step chemistry, to produce agreement of calculated ignition delays. Introduction of a criterion for inclusion of this correction factor, based on a test for the HO_2 steady state, results in a generally applicable three-step chemical-kinetic description for hydrogen-air combustion that possesses reasonable accuracy for most computational purposes.

Keywords: autoignition, reduced chemistry, hydrogen

1. Introduction

As computer power increases, reliance on the numerical computation of combustion processes is growing at the expense of experiment. To be confident in employing the numerical results, however, reasonable accuracy must be assured. One element in achieving this accuracy is to base the calculations on a correct detailed chemical-kinetic mechanism. This is more feasible for hydrogen-oxygen chemistry than for the oxidation of other fuels because fewer species and fewer elementary steps are involved for hydrogen. There are, in fact, only eight species and twenty one reversible elementary steps in the hydrogen oxidation mechanism, and the rate parameters for all of the steps are reasonably well known [1]. Despite this relative simplicity, combustion at high Reynolds numbers or in complex configurations excessively taxes computational capabilities even for hydrogen. This motivates the development of systematically reduced hydrogen-oxygen chemistry that has sufficient accuracy to yield reliable computational results.

Although a number of systematic reductions of hydrogen-oxygen mechanisms have been derived in the past, each is restricted to one particular combustion process. There are, for example, separate reductions for autoignition [2] and for laminar deflagration [3, 4]. A one-step overall mechanism, systematically derived for sufficiently lean deflagrations, is accurate for many purposes [5, 6]. Reductions for laminar diffusion flames [7, 8] are much more similar to those for deflagrations than to those for autoignition, although even the reductions for these flames exhibit differences in detail.

Reduced chemistry for detonations, on the other hand, would resemble that for autoignition more closely than that for flames.

What is needed for general computational approaches is sufficiently accurate reduced chemistry that encompasses all of these combustion processes because it is not known in advance, at the start of a calculation, in exactly what manner the combustion will develop. The purpose of the present investigation is to derive a systematically reduced description of hydrogen-oxygen chemistry that can be applied to all of these combustion processes with acceptable accuracy.

2. Description of the reduced mechanism

The so-called San Diego mechanism [1], used in the following development has been tested recently and for most conditions was shown to give excellent predictions for laminar flame burning velocities, induction time, oxidizer stream temperature at autoignition and strain rate at extinction. It consists of 21 reversible elementary reactions, involving 8 reacting species H_2, O_2, H_2O, H, O, OH, HO_2 and H_2O_2.

The reduction begins by noting that many of the elementary reactions have a negligible contribution to the reaction process, and can be therefore discarded in the first approximation, so that the twelve elementary reactions shown in Table 1, of which only six are reversible, suffice to describe premixed and nonpremixed flames, autoignition and detonations under conditions of practical interest. The table includes the reaction constants

	Reaction		A^a	n	E^a		A^a	n	E^a
1	$H+O_2 \rightleftharpoons OH+O$	k_f	$3.52\ 10^{16}$	-0.7	71.42	k_b	$7.04\ 10^{13}$	-0.26	0.60
2	$H_2+O \rightleftharpoons OH+H$	k_f	$5.06\ 10^{4}$	2.67	26.32	k_b	$3.03\ 10^{4}$	2.63	20.23
3	$H_2+OH \rightleftharpoons H_2O+H$	k_f	$1.17\ 10^{9}$	1.3	15.21	k_b	$1.28\ 10^{10}$	1.19	78.25
4	$H+O_2+M \rightarrow HO_2+M^b$	k_0	$5.75\ 10^{19}$	-1.4	0.0	k_∞	$4.65\ 10^{12}$	0.44	0.0
5	$HO_2+H \rightarrow 2OH$		$7.08\ 10^{13}$	0.0	1.23				
6	$HO_2+H \rightleftharpoons H_2+O_2$	k_f	$1.66\ 10^{13}$	0.0	3.44	k_b	$2.69\ 10^{12}$	0.36	231.86
7	$HO_2+OH \rightarrow H_2O+O_2$		$2.89\ 10^{13}$	0.0	−2.08				
8	$H+OH+M \rightleftharpoons H_2O+M^c$	k_f	$4.00\ 10^{22}$	-2.0	0.0	k_b	$1.03\ 10^{23}$	-1.75	496.14
9	$2H+M \rightleftharpoons H_2+M^c$	k_f	$1.30\ 10^{18}$	-1.0	0.0	k_b	$3.04\ 10^{17}$	-0.65	433.09
10	$2HO_2 \rightarrow H_2O_2+O_2$		$3.02\ 10^{12}$	0.0	5.8				
11	$HO_2+H_2 \rightarrow H_2O_2+H$		$1.62\ 10^{11}$	0.61	100.14				
12	$H_2O_2+M \rightarrow 2OH+M^d$	k_0	$8.15\ 10^{23}$	-1.9	207.62	k_∞	$2.62\ 10^{19}$	-1.39	214.74

Table 1: Rate coefficients in Arrhenius form $k = AT^n \exp\left(-E/R^oT\right)$, for the skeletal (12s) mechanism.

[a] Units are mol, s, cm^3, kJ, and K.

[b] Chaperon efficiencies are 2.5 for H_2, 16.0 for H_2O, and 1.0 for all other species; Troe falloff with $F_c = 0.5$

[c] Chaperon efficiencies are 2.5 for H_2, 12.0 for H_2O, and 1.0 for all other species.

[d] Chaperon efficiencies are 2.5 for H_2, 6.0 for H_2O, and 1.0 for all other species; $F_c = 0.265\exp\left(-T/94K\right) + 0.735\exp\left(-T/1756K\right) + \exp\left(-5182K/T\right)$

for the forward and backward rates as well as the chaperon efficiencies involved in reactions $4f$, 8, 9 and $12f$ and the rate parameters for the non-Lindemann pressure dependence of reactions $4f$ and $12f$. Skeletal mechanisms that contain fewer reactions can be used for specific combustion conditions. For instance, the submechanism formed by selecting the three shuffle reactions 1–3, the recombination reaction 4f and the HO_2 consuming reactions 5f, 6f and 7f, has been shown recently to describe accurately lean deflagrations [5]. The direct recombination reactions 8f and 9f need to be added if accuracy is required in describing stoichiometric and rich deflagrations as well as nonpremixed flames. Reaction $6b$ is responsible for the initial generation of radicals in the early induction stages of autoignition processes [9]. Additional initiation steps, such as $8b$ and $9b$ are not as important for initiation purposes, but they also need to be retained if chemical equilibrium at high temperature is to be properly described, a key factor in accurate computations of detonations. The H_2O_2 chemistry, on the other hand, is important to describe combustion for conditions that place the system at temperatures near or below the crossover temperature associated with the second explosion limit of hydrogen-oxygen mixtures, when the rate of radical production through the regular chain-branching/chain-terminating path controlled by reactions 1f and 4f becomes comparable to or smaller than that provided by reaction $12f$, as occurs for instance in deflagrations near the flammability limits. The elementary reactions $10f$ and $11f$ are responsible for H_2O_2 generation from HO_2, with the effect of the former being significant only in the absence of hydrogen, as occurs near the lean flammability limit.

The reduction continues by introducing steady-state assumptions for intermediates. The accuracy of the aproximation and the number of intermediates that can be assumed to be in steady state without excessive loss of accuracy depend on the combustion conditions. Thus, in deflagrations, steady state approximations can be assumed for OH, O and HO_2 [5], while the same approximation for H atoms would be very poor except near the lean flammability limit. In diffusion flames, the steady state assumption for OH is more accurate than that for O for the purpose of calculating critical ignition and extinction strain rates in counterflow configurations, but even imposing both of these steady states leads to errors in critical strain rates only of about 20% [8]. Thus errors approaching 20% for certain results must be accepted in imposing the O and OH steady states to achieve the reduced chemistry. In autoignition processes, on the other hand, a steady state assumption for HO_2 results in a poor approximation [9] and a steady

state approximation for H would apply only under extremely fuel-lean conditions, beyond normal flammability limits, while for O and OH it is accurate in fuel-rich systems [2]. As for the radical H_2O_2, its concentration is always sufficiently small for the steady-state approximation to be a very accurate representation under the conditions explored below.

The above considerations indicate that steady-state assumptions for O, OH and H_2O_2 can be introduced in seeking a reduced description that describes with reasonable accuracy premixed and nonpremixed flames together with autoignition processes. To identify the resulting reduced chemistry the equations expressing the production rate of the different chemical species $\dot{C}_i$ for the 12-step short mechanism can be combined linearly to give

$$\dot{C}_{H_2O} + \dot{C}_O + \dot{C}_{OH} + 2\dot{C}_{H_2O_2} = 2\omega_I \qquad (1)$$
$$\dot{C}_{O_2} = -\omega_I - \omega_{III}$$
$$\dot{C}_{H_2} - \dot{C}_{OH} - 2\dot{C}_O - 2\dot{C}_{H_2O_2} = \omega_{II} - \omega_{III} - 3\omega_I$$
$$\dot{C}_H + \dot{C}_{OH} + 2\dot{C}_O + 2\dot{C}_{H_2O_2} = 2\omega_I - 2\omega_{II} + \omega_{III}$$
$$\dot{C}_{HO_2} = \omega_{III},$$

where the rates

$$\omega_I = \omega_1 + \omega_{5f} + \omega_{10f} + \omega_{11f}$$
$$\omega_{II} = \omega_{4f} + \omega_8 + \omega_9 - \omega_{10f} - \omega_{11f} \qquad (2)$$
$$\omega_{III} = \omega_{4f} - \omega_{5f} - \omega_6 - \omega_{7f} - 2\omega_{10f} - \omega_{11f}$$

are related to those of the different elementary reactions. At steady state, the concentrations of the radicals O, OH and H_2O_2 are much smaller than those of the other species and their production rates $\dot{C}_O$, $\dot{C}_{OH}$ and $C_{H_2O_2}$ can be correspondingly neglected above, indicating that with the approximations introduced, the chemistry reduces to the three overall steps

$$3H_2 + O_2 \overset{I}{\rightleftharpoons} 2H_2O + 2H$$
$$H + H + M \overset{II}{\rightleftharpoons} H_2 + M$$
$$H_2 + O_2 \overset{III}{\rightleftharpoons} HO_2 + H$$
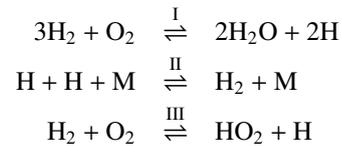
with global rates given in (2). Note that, although the reduced chemistry can be expressed in terms of different alternative sets of overall reactions, the resulting formulations are all equivalent. The one selected here is written in an intuitive form that serves to identify the main chemical processes involved in hydrogen combustion, i.e., it includes a branching reaction I, a recombination reaction II and an initiation reaction III.

The computation of the rates ω_{1b}, ω_{7f} and ω_{8f} requires knowledge of the concentrations of O and OH,

which can be obtained in explicit form by solving their steady-state equations $\dot{C}_O = \omega_1 - \omega_2 = 0$ and $\dot{C}_{OH} = \omega_1 + \omega_2 - \omega_3 + 2\omega_{5f} - \omega_{7f} - \omega_8 + 2\omega_{12f} = 0$ to give

$$C_{OH} = [(A_1^2 + 4A_0A_2)^{1/2} - A_1]/(2A_2) \qquad (3)$$

$$C_O = \frac{k_{1f}C_HC_{O_2} + k_{2b}C_{OH}C_H}{k_{1b}C_{OH} + k_{2f}C_{H_2}}. \qquad (4)$$

where

$$A_0 = C_{H_2}k_{2f}(2k_{1f}C_HC_{O_2} + k_{3b}C_HC_{H_2O} + 2k_{5f}C_HC_{HO_2}$$
$$+2k_{10f}C_{HO_2}^2 + 2k_{11f}C_{HO_2}C_{H_2} + k_{8b}C_{H_2O})$$
$$A_1 = +C_{H_2}k_{2f}(k_{8f}C_H + k_{7f}C_{HO_2} + k_{3f}C_{H_2})$$
$$-k_{1b}(k_{3b}C_HC_{H_2O} + 2k_{5f}C_HC_{HO_2}$$
$$+2k_{10f}C_{HO_2}^2 + 2k_{11f}C_{H_2O}C_{H_2} + k_{8b}C_{H_2O})$$
$$A_2 = k_{1b}(2k_{2b}C_H + k_{3f}C_{H_2} + k_{7f}C_{HO_2} + k_{8f}C_H).$$

3. Validation of the simplified chemistry descriptions
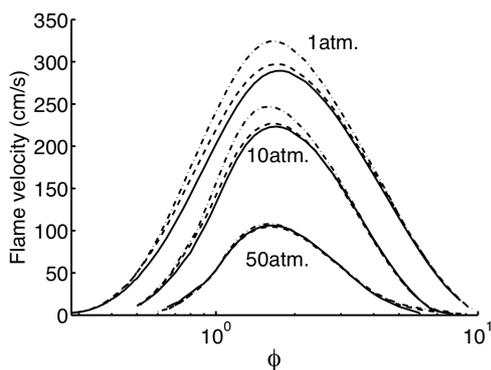
Figure 1: The variation with equivalence ratio of the laminar burning rate of hydrogen-air planar deflagrations with initial temperature $T_u = 300$ K and three different pressures as obtained with the detailed 21-step chemistry (solid curves), with the short 12-step chemistry (dashed curves) and with the 3-step reduced mechanism (dot-dashed curves).

Extensive computations of different H_2-air combustion configurations were performed to test the accuracy of the short and reduced mechanisms. For instance, the COSILAB code was used to compute steady planar deflagrations and nonpremixed counterflow flames with detailed transport descriptions including thermal diffusion. The results, including those shown in Figs. 1 and 2, indicate that the simplified mechanisms describe with sufficient accuracy burning rates and flammability limits in steady planar deflagrations as well as peak temperatures and extinction strain rates in nonpremixed

counterflow flames. For the reduced chemistry, the largest errors in predictions of flame propagation velocities, on the order of 12 %, are found at atmospheric pressure, whereas at higher pressures the steady-state assumptions present in the reduced chemistry become more accurate and yield better burning-rate predictions. The reduced chemistry also tends to overpredict peak temperatures in nonpremixed flames, giving departures on the order of 50 K for all strain rates, as seen in Fig. 2.
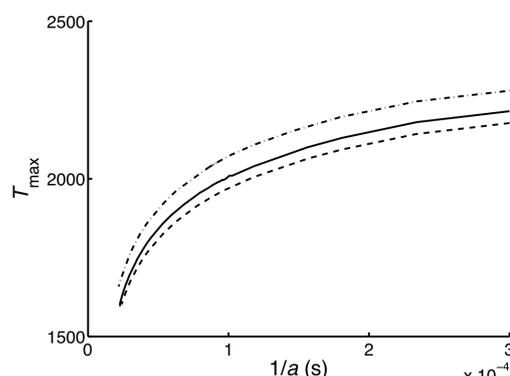
Figure 2: The variation with strain rate of the maximum temperature in a hydrogen-air planar counterflow at atmospheric pressure with feed-stream temperatures $T = 300$ K as obtained with the detailed 21-step chemistry (solid curves), with the short 12-step chemistry (dashed curves) and with the 3-step reduced mechanism (dot-dashed curves).

Besides laminar flames, two different autoignition configurations were used in computations. Figure 3 shows results of homogeneous adiabatic combustion in an isobaric reactor obtained with the COSILAB code at initial temperatures above crossover, with the ignition time defined in the computations by the temperature-inflection criterion. As can be seen, while the 12-step short description gives results that are virtually indistinguishable from those of the detailed chemistry, the 3-step mechanism is only accurate for fuel-rich conditions and give errors that are larger as the mixture becomes leaner. This necessitates the revisions for lean mixtures developed below.

The isobaric ignition histories computed in the transport-free homogeneous adiabatic reactor used in the computations of Fig. 3 apply in particular to the description of the induction region found downstream from the leading shock wave in detonations. Effects of molecular transport become important in describing autoignition in nonpremixed mixing layers [10], of interest in high-speed propulsion applications. To investigate the associated ignition process, the transient evolution
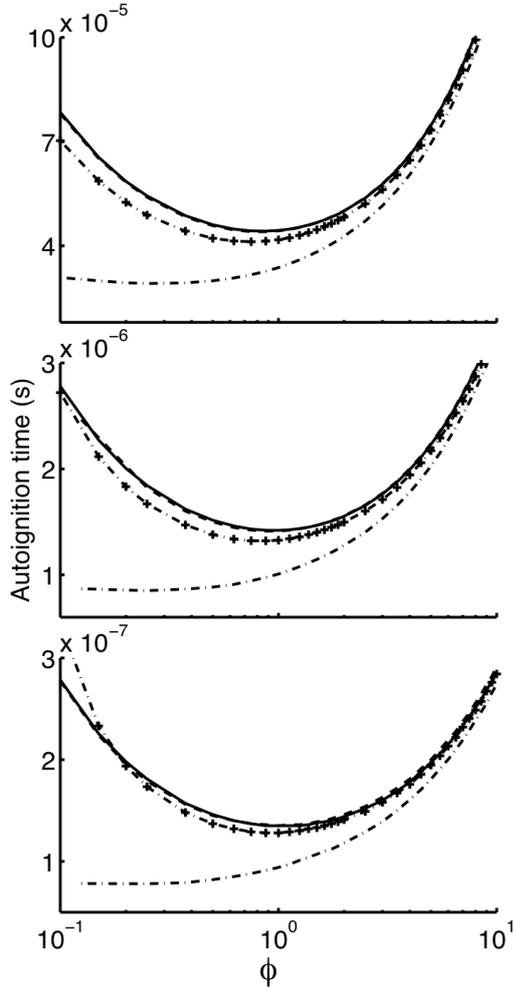
Figure 3: The variation with equivalence ratio of the induction time in isobaric homogeneous combustion for different conditions of pressure and initial temperature (upper plot: $T = 1200$ K and $p = 1$ atm; middle plot: $T = 1500$ K and $p = 10$ atm; lower plot: $T = 1800$ K and $p = 50$ atm) as obtained with the detailed 21-step chemistry (solid curves), with the short 12-step chemistry (dashed curves) and with the 3-step reduced mechanism (dot-dashed curves), with the crosses indicating the results obtained with the modified reaction-rate constant (9).

of a one-dimensional mixing layer formed by putting into contact at a given instant of time two semi-infinite spaces of hydrogen and air was investigated with use made of the NTMIX code [11]. If the initial temperature is sufficiently large, chemical reaction occurs as the reactants mix, giving rise to autoignition and to the formation of two premixed fronts that leave behind a trailing diffusion flame [12]. The resulting triple-flame structure can be observed in the plots of heat-release rate shown in Fig. 4 corresponding to an initial temperature $T = 1200$ K. As can be seen by comparing the results of the 21-step mechanism with those of the reduced chemistry, the errors in autoignition time present in Fig. 3 can also be observed here. The reduced chemistry predicts ignition to occur considerably earlier and at a point located farther into the air side of the mixing layer, in agreement with previous theoretical predictions [10].

4. The modified branching rate

The underpredictions of ignition times seen in Figs. 3 and 4 are too large for the associated reduced mechanism to provide an acceptable combustion description in the presence of autoignition. The errors are associated with the lack of accuracy of the steady-state assumptions for O and OH in the initial period of radical branching [9]. These assumptions are however excellent approximations when a sufficient radical pool has formed, e.g., within the reaction layer that controls the burning rate of premixed and nonpremixed flames. It is therefore of interest to seek ways to improve the description of autoignition with the reduced chemistry, without giving up the simplification associated with the steady-state assumptions of O and OH.

In autoignition events at temperatures above crossover, the chain-branching reactions $1f$ and $2f$ together with the chain-carrying reaction $3f$ control the autocatalytic radical growth after a short initial period in which the initiation reaction $6b$ creates the first radicals through collisions between the reactants [9]. The corresponding branched-chain explosion can be described with the effects of reactant consumption and heat release neglected in the first approximation by integrating the radical conservation equations

$$\begin{bmatrix} \dot{C}_H \\ \dot{C}_O \\ \dot{C}_{OH} \end{bmatrix} = \begin{bmatrix} -k_{1f}C_{O_2} & k_{2f}C_{H_2} & k_{3f}C_{H_2} \\ k_{1f}C_{O_2} & -k_{2f}C_{H_2} & 0 \\ k_{1f}C_{O_2} & k_{2f}C_{H_2} & -k_{3f}C_{H_2} \end{bmatrix} \cdot \begin{bmatrix} C_H \\ C_O \\ C_{OH} \end{bmatrix} \quad (5)$$

As shown in [9], the coefficient matrix possesses a single eigenvalue that is real and positive, λ, while the other two are complex conjugates with negative real
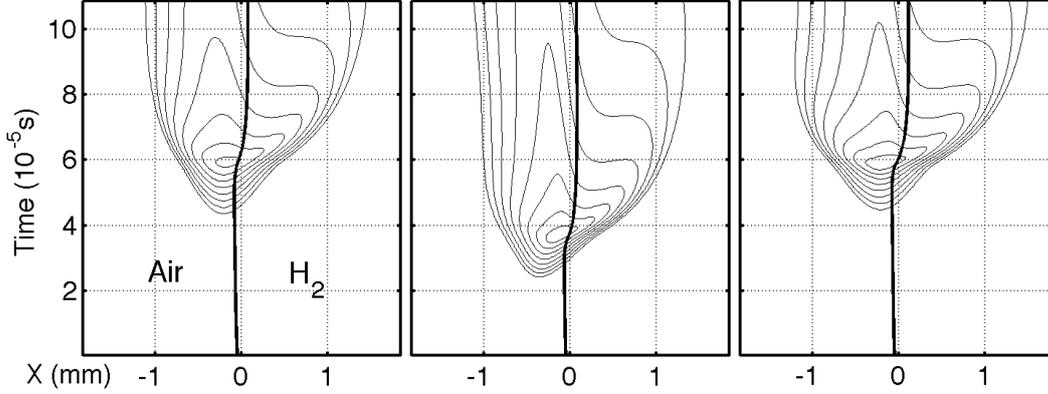
Figure 4: Isocontours of heat-release rate corresponding to $2^n \times 6.14 \times 10^7 \, J.m^{-3}.s^{-1}$ for $n = 0$ up to $n = 7$ in the transient one-dimensional H_2/air mixing layer at atmospheric pressure and initial temperature 1200K as obtained with the 21-step chemistry (left plot), with the 3-step reduced chemistry (centered plot) and with the modified 3-step reduced chemistry (right plot) ; the black line indicates the location where the mixture is stoichiometric.

parts, so that for large times the solution for the radical pool growth is given by integrating $dC/dt = \lambda C$ to give $C = C_i \exp(\lambda t)$, where C is the eigenvector associated with λ and the small factor C_i, proportional to k_{6b}, is the characteristic radical concentration during the initiation-controlled stage. The eigenvalue λ is determined as the solution of the characteristic equation associated with the coefficient matrix appearing in (5), giving a value that depends on the composition and temperature: it increases with increasing temperatures and, for a given temperature, reaches a maximum value at an intermediate equivalence ratio close to stoichiometric conditions. As shown in Fig. 5, the explicit expression

$$\lambda = 2k_{1f}C_{O_2}\Lambda \qquad (6)$$

with

$$\Lambda = [(1 + 2B)^{1/2} - 1]/B \qquad (7)$$

and

$$B = \frac{4k_{1f}C_{O_2}(k_{1f}C_{O_2} + k_{2f}C_{H_2} + k_{3f}C_{H_2})}{k_{2f}k_{3f}C_{H_2}^2}, \qquad (8)$$

obtained by neglecting the cubic term in the characteristic equation, is seen to give a very accurate representation for λ. It can be seen that for rich mixtures, such that $C_{H_2}/C_{O_2} \gg k_{1f}/k_{2f}$ and $C_{H_2}/C_{O_2} \gg k_{1f}/k_{3f}$, the eigenvalue simplifies to $\lambda \simeq 2k_{1f}C_{O_2}$, whereas the accompanying eigenvector reduces to $C \simeq C_H$, indicating that the H atom controls ignition, steady states for O and OH being reasonable for these rich conditions.

The exponential radical growth continues until radical-radical reactions, reactant consumption and heat
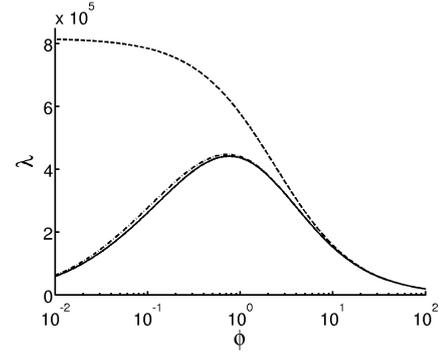
Figure 5: The variation with composition of λ at $T = 1200$ K and $p = 1$ atm (solid curve) together with the approximate solutions $\lambda = 2k_{1f}C_{O_2}$ (dashed curve) and $\lambda = 2k_{1f}C_{O_2}\Lambda$ (dot-dashed curve).

release become significant, as the radical concentrations reach sufficiently large values, comparable to the initial reactant concentrations. Therefore, the ignition time is given in the first approximation by $t_i = \lambda^{-1}\ln(\varepsilon^{-1})$ where ε, typically on the order of 10^{-6}, is the characteristic radical mole fraction at the end of the initiation period. This ignition time is to be compared with that predicted with the reduced chemistry, which, with O and OH in steady state, is determined by integrating the H-atom conservation equation $\dot{C}_H = 2\omega_I - 2\omega_{II} + \omega_{III}$, which reduces to $dC_H/dt = 2k_{1f}C_{O_2}C_H$ during the ignition period at temperatures above crossover. The resulting radical exponential growth $C_H \propto \exp(2k_{1f}C_{O_2}t)$ differs in general from that determined above for the radical pool $C \propto \exp(\lambda t)$, except for very rich mixtures,

for which $\lambda \simeq 2k_{1f}C_{O_2}$ and $C \simeq C_H$, as previously discussed. Correspondingly, the ignition time obtained with the reduced chemistry is a factor $\Lambda = \lambda/(2k_{1f}C_{O_2})$ smaller than that obtained by integrating the initial problem (5), which explains the differences observed in Figs. 3 and 4.

The above discussion suggests that these large errors, associated with the steady-state assumptions for O and OH present in the reduced chemistry, can be avoided by introducing a modified reaction-rate constant

$$k_{1f}^* = \Lambda k_{1f}, \tag{9}$$

where the factor Λ is defined in (7) and (8) as a function of the local temperature and composition. The accuracy associated with this correction is illustrated in Fig. 3, which includes reduced-chemistry ignition-time computations obtained with the modified reaction-rate constant (9).

5. The modification criterion

The modified rate applies to the description of the rapid chain-branching radical growth that leads to autoignition, but it must be switched off by setting $\Lambda = 1$ in places where the steady-state assumptions for O and OH apply with sufficient accuracy, which occur in general in hot regions with relatively high radical concentrations. To complete the correction to the reduced chemistry for general use then a simple criterion is needed that can be employed to identify chain-branching radical explosions automatically in numerical computations of complex reactive flows. For the three-step reduced chemistry, the steady-state approximation of the hydroperoxyl radical HO_2 can be used for that purpose. Under most conditions, in places where the chemical reaction is significant, the H and OH concentrations are sufficiently large for reactions $5f$, $6f$ and $7f$ to maintain the HO_2, produced mainly by reaction $4f$, in steady state. As previously observed [9], this does not occur, however, where autoignition is taking place. In a general computation, therefore, one may identify the places where autoignition is possibly occuring - and where the modified reaction-rate constant (9) is therefore needed - by checking the validity of the steady-state assumption for HO_2. For that purpose, the rate of HO_2 production $\dot{C}_{HO_2P} = \omega_{4f} + \omega_{6b}$ and that of HO_2 consumption $\dot{C}_{HO_2C} = \omega_{5f} + \omega_{6f} + \omega_{7f} + 2\omega_{10f} + \omega_{11f}$ are computed locally. The steady-state is regarded as a valid approximation wherever $|\dot{C}_{HO_2P} - \dot{C}_{HO_2C}|/\dot{C}_{HO_2P}$ is smaller than a presumed threshold value, below which $\Lambda = 1$

in (9), whereas for larger values the corrected reaction-rate constant must be employed, since autoignition may be occurring.

The results obtained with use of this simple triggering criterion were found to be quite independent of the threshold value used, provided the value selected was sufficiently small. In particular, it was observed that when a threshold value $|\dot{C}_{HO_2P} - \dot{C}_{HO_2C}|/\dot{C}_{HO_2P} = 0.05$ is employed, the modification introduced does not affect the results of computations of steady planar deflagrations and counterflow diffusion flames, which remain virtually identical to those determined without the correction, because the steady-state assumption for HO_2 applies in these flames within the reaction region, so that the modified rate is not triggered there. On the other hand, the description of mixing-layer autoignition is considerably improved when the modified reaction rate is employed with the same threshold value $|\dot{C}_{HO_2P} - \dot{C}_{HO_2C}|/\dot{C}_{HO_2P} = 0.05$, as can be seen in the right plot of Fig. 4.

6. Conclusions

The principal objectives of most computational studies of hydrogen-air combustion are to predict temperatures, pressures and concentrations of major species as functions of space and time. The detailed chemistry involves only 21 reversible elementary steps among 8 chemical species, resulting, in view of the two atom-conservation equations, in a mechamism which in principle involves only 6 overall steps [1, 2], but even this mechanism often is too large to be handled computationally in a convenient manner. It has been shown here that the principal objectives can be met by a 12-step elementary mechanism in which only 6 of the elementary steps are reversible, as well as by a systematically derived 3-step overall mechanism based on steady-state approximations for O, OH and H_2O_2, with the specific reaction-rate constant for the main elementary branching step modified to improve autoignition-time agreements under fuel-lean and stoichiometric conditions, for which the hypothesized O and OH steady states fail. Inaccurate representations of minor-species concentrations may be anticipated in certain regions from this reduced chemistry, but for deflagration, detonation and ignition and extinction studies in which interest focuses on gasdynamic, transport and heat-release processes, extending to both low-speed and supersonic combustion, these simplified descriptions may enable sufficiently accurate calculations to be performed that otherwise would not be possible.

Acknowledgements

[1] P. Saxena, F.A. Williams, Combust. Flame, 145 (2006) 316–323. Also available at http://maemail.ucsd.edu/combustion/cermech.

[2] F.A. Williams, J. Loss Prev. Proc. Indust., 21 (2008) 131–135.

[3] F. Mauss, N. Peters, B. Rogg, F. A. Williams, in: Reduced Kinetic Mechanisms for Applications in Combustion Systems, N. Peters, B. Rogg, (Eds.) Springer-Verlag, Heidelberg, 1993, pp. 29–43.

[4] K. Seshadri, N. Peters, F. A. Williams, Combust. Flame 96 (1994) 407–427.

[5] D. Fernández-Galisteo, A.L. Sánchez, A. Liñán, F. A. Williams *Combust. Flame* 156 (2009) 985–996.

[6] D. Fernández-Galisteo, A.L. Sánchez, A. Liñán, F. A. Williams *Combust. Th. Modelling* 13 (4) (2009) 741–761.

[7] E. Guthiel, G. Balakrishnan, F.A. Williams, in: Reduced Kinetic Mechanisms for Applications in Combustion Systems, N. Peters, B. Rogg, (Eds.) Springer-Verlag, Heidelberg, 1993, pp. 177-195.

[8] G. Balakrishnan, M.D. Smooke, F.A. Williams, Combust. Flame,102 (1995) 329–340.

[9] G. del Alamo, F.A. Williams, A.L. Sanchez, Combust. Sci. Tech. 176 (2004) 1599–1626.

[10] A.L. Sánchez, A. Liñán, F. A. Williams, SIAM J. Appl. Math. 59 (1999) 1335-1355.

[11] M. Baum, D. Haworth, T. Poinsot, N. Darabiha, J. Fluid Mech. 281 (1994) 1–32.

[12] A. Liñán, A. Crespo, Combust. Sci. Tech. 14 (1976) 95–117.